Bulk moduli and high-pressure crystal structures of the mixed valent compound Pb_3O_4 determined by X-ray powder diffraction

R.E. Dinnebier; S. Carlson (MAX-lab, Lund); M. Hanfland (ESRF, Grenoble); M. Jansen

In chemical compounds exhibiting significant covalent bonding contributions, 'lone', i.e., non-bonding, electron pairs can be strongly stereochemically active. Generally they are regarded as pseudo-ligands that are able to replace one or more of the regular ligands in a given coordination sphere. The resulting stereochemical implications have been discussed in depth, and the model derived has also been applied to extended solids. In parallel to the strong geometric effects, also the physical properties are affected. The anisotropic local environments of those atoms bearing a 'lone-pair' in their valence shells frequently induce the formation of acentric or even polar crystal structures, leading to the known consequences for the dielectric properties. Since the structures formed are rather open, and cations with 'lone-pairs' exhibit high polarizabilities, such compounds showing lone-pair related structural features should be highly susceptible to undergo pressure induced phase transitions. Geometric and electronic structures of solids are strongly correlated. Thus, at a transformation to a reorganized structure of higher density one would expect significant consequences also for the electronic structure.

Several different scenarios can be imagined: (1) The 'lone-pair' could be forced into a pure *s*-type state, removing all anisotropies in the coordination sphere. (2) The valence band (in most instances also including the non-bonding electron pair) and the conduction band will broaden or even overlap, leading to semiconducting or metallic behavior, respectively. (3) In case of mixed valent representatives the originally localized lone-pair might delocalize, making the valence states of the respective metal ions indiscernible and producing a partially filled band at the Fermi level, again leading to metallic behavior. Recently, the latter situation has attracted high attention, in the context of trying to understand superconductivity observed in oxides containing metal ions featuring 'lone-pairs'. The theoretical models suggest that superconductivity in such compounds may be induced by applying high external pressure. In the context of the above considerations the industrially important mixed valent lead tetroxide Pb_3O_4 (minium) appeared to be a good candidate for probing such an approach.

Minium is considered a member of the Spinel group of oxide minerals although the crystal structures are quite different. In minium, the lead occurs in two different valence states $(Pb^{+4})(Pb^{+2})_2O_4$, where the free electron pair of Pb^{+2} can be considered as an additional ligand causing severe distortions of the coordination polyhedra. Minium is a semiconductor with a bandgap of 2.1(1) eV which has been confirmed experimentally (reflectance and photovoltaic technique) and also theoretically (augmented spherical wave method). At room temperature, minium crystallizes in space group $P4_2/mbc$. Upon cooling a displazive phase transition at 270 K towards an orthorhombic phase (space group *Pbam*) was found, while upon heating, minium undergoes two additional ferroelectric, respective ferroelastic displazive phase transitions from to non-centrosymmetric orthorhombic, at 195 K to non-centrosymmetric tetragonal and finally at 225 K to $P4_2/mbc$.

In this work, we have investigated the pressure dependence of the crystal structure of Pb_3O_4 which we consider a prerequisite for future investigations of the transport properties of Pb_3O_4 under lasting pressure or possible quenched high-pressure modifications. For this purpose, *in situ* X-ray powder diffraction measurements were performed at room temperature and elevated pressures at room temperature at beamline ID9 of the European Synchrotron Radiation Facility (ESRF) using a diamond anvil cell.

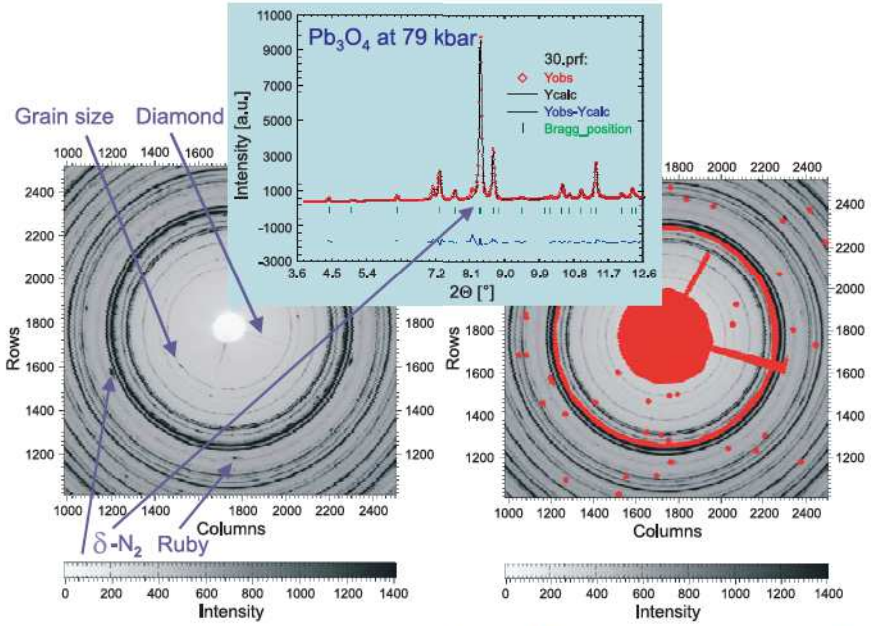

Figure 90: Data reduction and integration of Debye-Scherrer rings for Pb_3O_4 at 7.9 GPa.

Diffracted intensities were recorded with a Marresearch Mar345 online image plate system in the pressure range from 0.06 to 41.05 GPa (Figs. 90 and 91). The dependence of the scattering profile on pressure gives evidence for two second order phase transitions (Fig. 91).

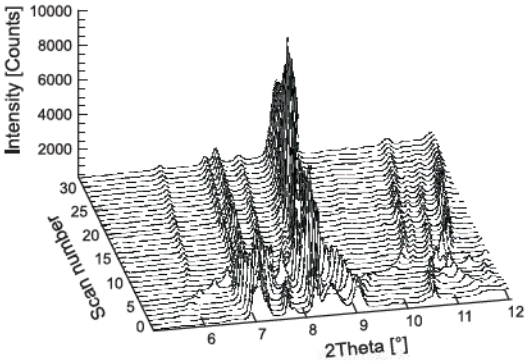

Figure 91: Scattered X-ray intensity of Pb_3O_4 as a function of diffraction angle 2Θ and pressure (non-linear pressure scale from scan number 0 at 0 GPa to scan number 32 at 41.05 GPa). The wavelength was $\lambda = 0.41594$ Å. Phases identified are in order of increasing pressure:
(I) $P4_2/mbc$ ($0 < P \leq 0.12$ GPa),
(II) *Pbam* ($0.3 \leq P \leq 5.54$ GPa),
(III) *Pbam* ($c' = c/2$) ($6.59 \leq P \leq 41.05$ GPa).

The phase with tetragonal symmetry ($P4_2/mbc$) (phase I) which is stable at ambient conditions is retained up to at least 0.11 GPa. A transition into a phase with orthorhombic symmetry (*Pbam*) (phase II) is observed to occur between 0.11 GPa and 0.3 GPa which is stable to at least 5.54 GPa. Between 5.54 and 6.58 GPa a second phase transition occurs to another orthorhombic phase (*Pbam*; halved *c*-axis) (phase III) which stays stable until at least 41.05 GPa (Fig. 92). The quality of the powder patterns of phases I and II was sufficient to extract lattice parameters and to verify the crystal structures via Rietveld refinement. All powder patterns of phase III (Fig. 92) contained sufficiently resolved diffraction peaks to allow for *ab initio* crystal structure determination using direct methods in combination with difference-Fourier analyses.

X-ray scattering on Pb_3O_4 has provided the lattice parameters and unit cell volume as a function of pressure (Fig. 93). The volume V decreases by 32% at 41 GPa, indicating a very soft and highly compressible material. The volume / pressure relation represents the equation

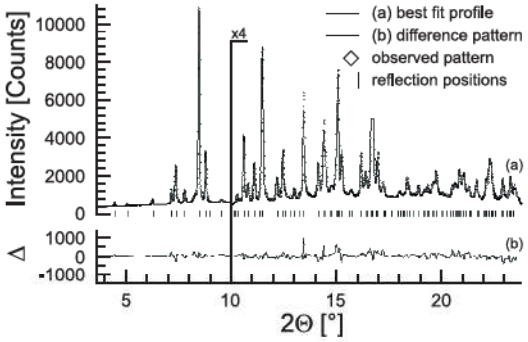

Figure 92: Rietveld plot of the high-pressure phase III of Pb_3O_4 in *Pbam* at $P = 13.2$ GPa as a function of diffraction angle 2Θ. The wavelength was $\lambda = 0.41594$ Å. The higher angle part starting at 10.0° 2Θ is enlarged by a factor of 4. The *R*-values are *R*-p = 2.5%, *R*-wp = 3.8%, and *R*-F^2 = 9.3%.

of state (EoS) which was described by the Vinet EoS which is believed to yield more accurate parameters for highly compressible materials. Two dashed lines drawn through the volume data in Fig. 93 represent the fitted Vinet EoS. The bulk modulus of phase II in comparison to the corresponding values of phase III is about 4.7 times lower indicating a much higher compressibility. This behavior can be related to packing effects of the Pb^{2+} polyhedra at low pressure due to a change in space requirement of the free electron pair. According to a hard sphere model, the space filling at ambient conditions (phase I) is only 44.2%, which is far away from a closed packed structure, and it increases rapidly until the stable high-pressure phase III (60% at 13.3 GPa) is reached. The pressure dependence of the lattice parameters shows a distinct anisotropy, which reflects the space requirements of the free electron pair of Pb^{2+}.

From the Rietveld refinements of the powder patterns of phases I and II at high pressure it can be concluded that they are isostructural to their counterparts at low temperature. In particular the high-quality of the powder patterns of the previously unknown phase III of minium permitted high-quality Rietveld refinements and therefore allowed the accurate determination of structural parameters in dependence on pressure.

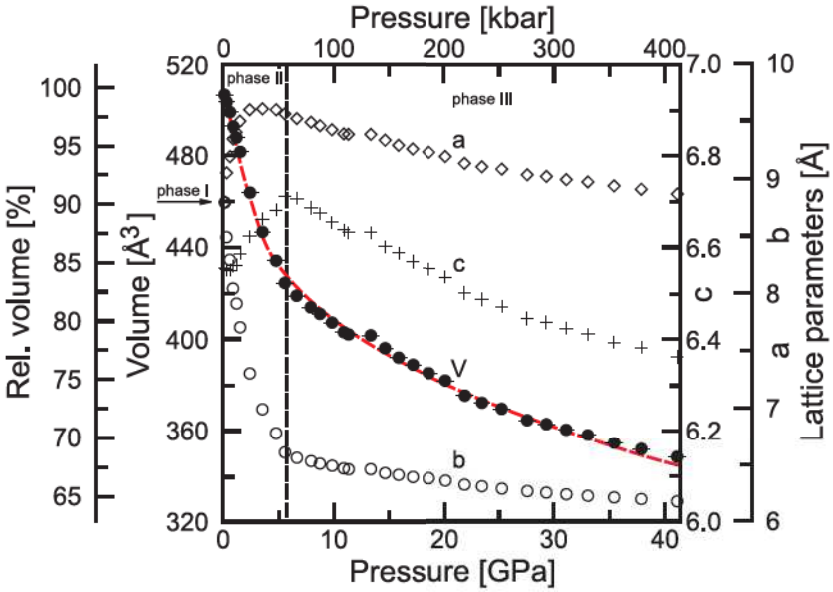

Figure 93: Dependence of the lattice parameters, volume, and relative volume of Pb_3O_4 on pressure in the range of 0–41.05 GPa. The high-pressure phase transition between the two orthorhombic phases (II, III) at approximately 6 GPa is marked by a vertical dashed line. For better comparison, the *c*-axis of phase III is doubled. The dashed fitted lines correspond to least squares fits of Vinet equations of state for the two orthorhombic phases (II, III).

The basic crystal packing of phases I/II is still preserved in phase III of minium (Figs. 94, 95). Phase III forms in the moment as the external pressure is strong enough to flatten the Pb^{2+}–tetrahedral (phase I) resp, orthorhombic bisphenoids (phase II) to rectangular sheets, making the two different Pb^{2+} sites crystallographically indistinguishable again, leading to an unexpected increase of symmetry at higher pressure. The main difference of the crystal structure of minium at pressures above 6.58 GPa is the increase of the coordination number of Pb^{2+} from 4 to 6+1, forming distorted $Pb^{2+}O_7$ trigonal prisms with a pyramidal vertex on one of the rectangular planes (Fig. 94). The packing may be viewed as a strongly distorted hexagonal closed packing (hcp) arrangement leading to the formula $(Pb^{+4}\square_3)^{VI}\,(Pb_2^{+2}\square_6)^{IV}O_4$. The resulting crystal structure is of Sr_2PbO_4 aristotype.

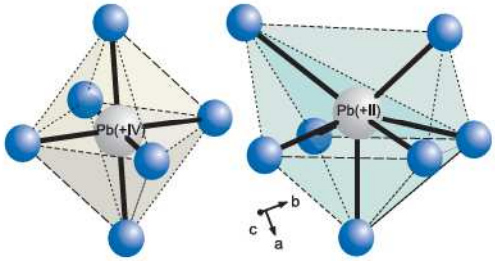

Figure 94: Regular $Pb^{+4}O_6$ octahedron (left) and irregular $Pb^{+2}O_{6+1}$ capped trigonal prism (right) in Pb_3O_4 at 13.3 GPa (phase III).

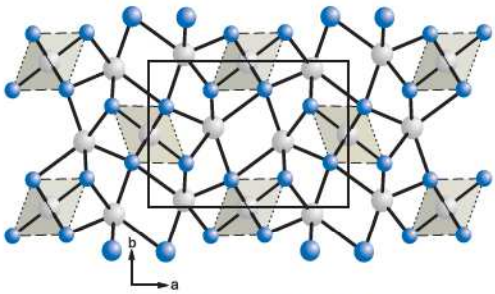

Figure 95: Ball and stick model of the crystal structure of Pb_3O_4 at 13.3 GPa (phase III) in a projection along *c*-axis. The $Pb^{+4}O_6$ octahedra are shown.

Small differences between the crystal structures of Pb_2PbO_4 (phase III) and Sr_2PbO_4 are due to different distortions of the $Pb^{2+}O_7$ respectively $Sr^{2+}O_7$ polyhedra. This can be explained by sterical requirements of the lone pair of lead (II). Whereas the long metal-oxygen bond in the $Sr^{2+}O_7$ polyhedron connects the oxygen atom at the pyramidal vertex with the central cation (2.99 Å), it is an oxygen atom at the roof of the trigonal prism in case of $Pb^{2+}O_7$ polyhedron (2.95 Å) (Fig. 94). The small deviations of the central cations from the centers of gravity of the capped trigonal prism is basically identical (0.25–0.30 Å) for both compounds.

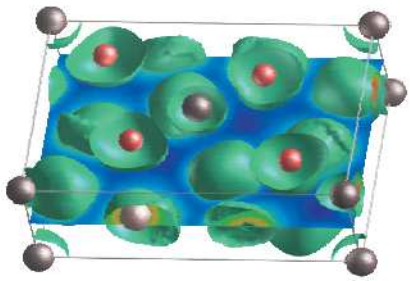

Figure 96: Isosurface of the electron localization function (ELF = 0.385) for Pb_3O_4 at 13.3 GPa (phase III).

This structural relationship is clearly indicating that the stereochemical needs of Pb^{2+} under high pressure are similar to those of Sr^{2+}. Thus the response of the electronic structure to the external pressure follows scenario (1), as outlined in the introduction, and the lone pair has adopted an almost pure *s*-type which is further supported by the similarity of the $Sr^{2+}O_{6+1}$ and $Pb^{2+}O_{6+1}$ coordination polyhedra. Furthermore, the volume increment per oxygen atom for Pb_3O_4 at 13.3 GPa is close to the values found for Sr_2PbO_4 exhibiting no lone pair, and is significantly lower than that of Pb_3O_4 at ambient conditions and of β-PbO. Whereas in case of Pb_3O_4 (phase I) the packing densities are close to that of β-$Pb^{2+}O$ (41%) due to the sterical requirements of the lone pairs, the packing densities for β-$Pb^{4+}O_2$, Sr_2PbO_4 and Pb_3O_4 (phase III at 13.3 GPa) are with 60 to 62% typical for close packed structures, showing no signs of stereocative lone pairs. The remaining lone pair of Pb_3O_4 at 13.3 GPa is visualized by the isosurface of the electron localization function (Fig. 96).